

 Open access • Journal Article • DOI:10.1007/S10569-010-9256-8

Effects of Interplanetary Dust on the LISA drag-free Constellation — [Source link](#)

Massimo Cerdonio, Fabrizio De Marchi, Roberto De Pietri, Philippe Jetzer ...+5 more authors

Institutions: University of Padua, University of Trento, University of Parma, University of Zurich ...+2 more institutions

Published on: 02 Feb 2010 - arXiv: General Relativity and Quantum Cosmology

Topics: Gravitational field, Interplanetary dust cloud, Zodiacal light, Dark matter and Solar System

Related papers:

- [Effects of interplanetary dust on the LISA drag-free constellation](#)
- [Relativistic analysis of the LISA long range optical links](#)
- [On the detection of gravitational radiation by the Doppler tracking of spacecraft.](#)
- [Asteroid perturbations and the possible determination of asteroid masses through the ASTROD space mission](#)
- [A new approach to applying interplanetary meteoroid flux models to spacecraft in gravitational fields](#)

Share this paper:    

View more about this paper here: <https://typeset.io/papers/effects-of-interplanetary-dust-on-the-lisa-drag-free-3ynp6ivs0u>



**University of
Zurich**^{UZH}

**Zurich Open Repository and
Archive**

University of Zurich
University Library
Strickhofstrasse 39
CH-8057 Zurich
www.zora.uzh.ch

Year: 2010

Effects of interplanetary dust on the LISA drag-free constellation

Cerdonio, M ; de Marchi, F ; de Pietri, R ; Jetzer, P ; Marzari, F ; Mazzolo, G ; Ortolan, A ; Sereno, M

Abstract: The analysis of non-radiative sources of static or time-dependent gravitational fields in the Solar System is crucial to accurately estimate the free-fall orbits of the LISA space mission. In particular, we take into account the gravitational effects of Interplanetary Dust (ID) on the spacecraft trajectories. The perturbing gravitational field has been calculated for some ID density distributions that fit the observed zodiacal light. Then we integrated the Gauss planetary equations to get the deviations from the LISA Keplerian orbits around the Sun. This analysis can be eventually extended to Local Dark Matter (LDM), as gravitational fields are expected to be similar for ID and LDM distributions. Under some strong assumptions on the displacement noise at very low frequency, the Doppler data collected during the whole LISA mission could provide upper limits on ID and LDM densities. Cerdonio, Massimo; de Marchi, Fabrizio; de Pietri, Roberto; Jetzer, Philippe; Marzari, Francesco; Mazzolo, Giulio; Ortolan, Antonello; Sereno, Mauro

DOI: <https://doi.org/10.1007/s10569-010-9256-8>

Posted at the Zurich Open Repository and Archive, University of Zurich

ZORA URL: <https://doi.org/10.5167/uzh-34382>

Journal Article

Accepted Version

Originally published at:

Cerdonio, M; de Marchi, F; de Pietri, R; Jetzer, P; Marzari, F; Mazzolo, G; Ortolan, A; Sereno, M (2010). Effects of interplanetary dust on the LISA drag-free constellation. *Celestial Mechanics and Dynamical Astronomy*, 107(1-2):255-264.

DOI: <https://doi.org/10.1007/s10569-010-9256-8>

Effects of Interplanetary Dust on the LISA drag-free Constellation

Massimo Cerdonio, Fabrizio De Marchi,
Roberto De Pietri, Philippe Jetzer, Francesco
Marzari, Giulio Mazzolo, Antonello Ortolan
and Mauro Sereno

the date of receipt and acceptance should be inserted later

Abstract The analysis of non-radiative sources of static or time-dependent gravitational fields in the Solar System is crucial to accurately estimate the free-fall orbits of the LISA space mission. In particular, we take into account the gravitational effects of Interplanetary Dust (ID) on the spacecraft trajectories. The perturbing gravitational field has been calculated for some ID density distributions that fit the observed zodiacal light. Then we integrated the Gauss planetary equations to get the deviations from the LISA keplerian orbits around the Sun. This analysis can be eventually extended

M. Cerdonio and F. Marzari
Department of Physics, University of Padova and INFN Padova, via Marzolo 8, I-35131 Padova, Italy

F. De Marchi
Department of Physics, University of Trento and INFN Trento, via Sommarive 14, I-38123 Povo (Trento), Italy

R. De Pietri
Department of Physics, University of Parma and INFN Parma, I-43100 Parma, Italy

Ph. Jetzer
Institute of Theoretical Physics, University of Zürich, Winterthurerstrasse 190, CH-8057 Zürich, Switzerland

G. Mazzolo*
Max Planck Institut für Gravitationsphysik, Callinstrasse 38, 30167 Hannover, Germany
*To whom address correspondence: giulio.mazzolo@aei.mpg.de

A. Ortolan
INFN Laboratori Nazionali di Legnaro, Viale dell'Università 2, I-35020 Legnaro (Padova), Italy

M. Sereno
Institute of Theoretical Physics, University of Zürich, Winterthurerstrasse 190, CH-8057 Zürich, Switzerland and Department of Physics, Politecnico di Torino, Corso Duca degli Abruzzi 24, 10129 Torino, Italy

to Local Dark Matter (LDM), as gravitational fields are expected to be similar for ID and LDM distributions. Under some strong assumptions on the displacement noise at very low frequency, the Doppler data collected during the whole LISA mission could provide upper limits on ID and LDM densities.

Keywords LISA · interplanetary dust · dark matter · gravitational waves

1 Introduction

LISA (Laser Interferometer Space Antenna) is a joint space mission by ESA and NASA which is planned to be launched at the end of the next decade. It consists of three identical free-falling satellites, orbiting around the Sun and marking the vertices of a nearly equilateral triangle with $\simeq 5 \cdot 10^6$ km (1/30 AU) sides, located 20° behind the Earth and lying in a plane that makes an angle of 60° with the ecliptic [2]. LISA target is the detection of gravitational waves (GWs) through the measure of the relative and differential motions between the spacecrafts. Among the astrophysical goals of LISA is to detect GWs originated by events like black holes coalescence or capture of compact objects by black holes [3]. This requires a strain sensitivity of $10^{-20} \text{ Hz}^{-1/2} < S_h^{1/2} < 10^{-17} \text{ Hz}^{-1/2}$ in the 10^{-4} to 10^{-1} Hz frequency band range.

However, LISA reference masses interact also with time-dependent (e.g. planets and their satellites, quadrupolar pulsation of the Sun, etc.) and static (e.g. ID and LDM) local gravitational fields, and therefore they depart from ideal unperturbed orbits around the Sun. In this paper, we focused on the perturbing effects caused by the static components ID and LDM. As the discriminating feature between ID and LDM concerns only their coupling with the electromagnetic field, we expect that ID and LDM will produce similar gravitational forces on reference masses¹. In fact, only ID reflects the solar light and can be studied through observations of zodiacal light [9], while LDM is “dark” and its presence can be investigated by means of gravitational perturbations induced on orbiting bodies. It is worth mentioning that other possibilities for detection of DM are the searches for particular electro-weak processes beyond the Standard Model at particle colliders. Thus we assume that ID and LDM induce identical gravitational effects on LISA orbits, with the irrelevant difference that the first is luminous and the second is dark.

As we will show, the linear perturbation theory holds, being other gravitational forces acting on LISA reference masses much smaller than the Sun pull; under this approximation, small perturbations to ideal keplerian motions induced by different sources in the Solar System can be studied separately.

2 Interplanetary dust

The ID cloud is a dust composed by grains with typical sizes of $10 - 100 \mu\text{m}$ pervading the Solar System. The distribution of ID particles is studied by the observations of solar light scattering (i.e. the zodiacal light confined to the ecliptic plane) and by their

¹ This is correct only in Newtonian physics: in fact, DM and ID are expected to be gravitationally bound to the Galaxy and to the Solar System respectively; therefore, while gravitoelectric effects are identical for the two, that would not be the case for the gravitomagnetic ones, i.e., effects depending on the speed of the considered objects.

thermal emission, which is the dominant component of night-sky light in the $5 - 50 \mu\text{m}$ wavelength [14]. Physical models of ID density distribution ρ should account for its symmetries, that can be easily described in the Solar System Baricentric (SSB) reference frame (x, y, z) : i) invariance under rotation about the z axis, and ii) invariance under reflections in the (x, y) ecliptic plane². Usually one also assumes a static distribution and a power-law radial profile. As a consequence, all the proposed models factorize ρ into two functions [9]

$$\rho(r, \beta_{\odot}) = \rho_0 \left(\frac{r_0}{r} \right)^{\alpha} f(\beta_{\odot}), \quad (1)$$

where r is the distance from the Sun, β_{\odot} is the heliocentric latitude, $\rho_0 \simeq 9.6 \times 10^{-20} \text{ kg/m}^3$ is the density value at $r_0 = 1 \text{ AU}$ (Earth's orbit), as estimated by the integration of the meteoroid mass distribution far away from the Earth, in order to avoid its gravitational attraction on ID particles, and f is a given function. The typical value of the parameter α , determined from zodiacal light photometer measurements on Helios 1 and 2 [10], is 1.3.

The expression of $f(\beta_{\odot})$ is still uncertain; however, the analytical formula which best reproduces the observations of zodiacal light is the so-called *ellipsoid model*

$$\rho(r, \beta_{\odot}) = \rho_0 \left(\frac{r_0}{r} \right)^{\alpha} \frac{1}{[1 + (\gamma_E \sin \beta_{\odot})^2]^{\alpha/2}}, \quad (2)$$

where $\gamma_E = \sqrt{a^2 - b^2}/b$, a and b are the semi-major and semi-minor axes of an oblate ellipsoid respectively. Beyond $\sim 3 \text{ AU}$ in the ecliptic plane and $\sim 1.5 \text{ AU}$ off the ecliptic plane, no reliable density values can be obtained from the zodiacal light. Therefore we assume $a = 3 \text{ AU}$ and $b = 1.5 \text{ AU}$ for the semi-axes and $\gamma_E = \sqrt{3}$ [9]. It is worth noticing that the total ID mass amount inside the considered region is of the order of 10^{17} kg , i.e., $\approx 10^{-8} M_{\oplus}$.

The ellipsoid model of ID density depends on two parameters, α and γ_E , and, in order to numerically study gravitational effects of ID on LISA orbits, we will consider four cases: i) *spherical homogeneous distribution* ($\alpha = 0, \gamma_E = 0$), ii) *spherical distribution with power-law density profile* ($\alpha = 1.3, \gamma_E = 0$), iii) *ellipsoidal homogeneous distribution* ($\alpha = 0, \gamma_E = \sqrt{3}$), and iv) *ellipsoidal distribution with power-law density profile* ($\alpha = 1.3, \gamma_E = \sqrt{3}$).

3 Method

As the first step we define the unperturbed LISA orbits³. The cartesian coordinates of each LISA reference mass ($k = 1, 2, 3$) are related to the keplerian orbital elements defined in the SSB through the following equations:

² The distribution is not symmetric with respect to the ecliptic plane, but to one defined by the total angular momentum of the Solar System. The differences between the two planes are negligible for our scopes.

³ In this paper we neglect post-Newtonian and relativistic effects.

$$\begin{cases}
x_k(t) = a_k [(\cos \Omega_k \cos \omega_k - \sin \Omega_k \sin \omega_k \cos i_k) (\cos \psi_k(t) - e_k)] \\
\quad + a_k \left[(-\cos \Omega_k \sin \omega_k - \sin \Omega_k \cos \omega_k \cos i_k) \sqrt{1 - e_k^2} \sin \psi_k(t) \right] \\
y_k(t) = a_k [(\cos \Omega_k \cos \omega_k + \sin \Omega_k \sin \omega_k \cos i_k) (\cos \psi_k(t) - e_k)] \\
\quad + a_k \left[(-\sin \Omega_k \sin \omega_k + \cos \Omega_k \cos \omega_k \cos i_k) \sqrt{1 - e_k^2} \sin \psi_k(t) \right] \\
z_k(t) = a_k \left[\sin \omega_k \sin i_k (\cos \psi_k(t) - e_k) + \cos \omega_k \sin i_k \sqrt{1 - e_k^2} \sin \psi_k(t) \right],
\end{cases} \quad (3)$$

where a_k is the semi-major axis, e_k the eccentricity, i_k the inclination of the orbit with respect to the ecliptic plane, ω_k the argument of periapsis, Ω_k the longitude of ascending node and $\psi_k(t)$ the eccentric anomaly [6]. We chose the initial conditions providing rigid triangular configuration of side $l \simeq 5 \times 10^6$ km $\simeq 1/30$ AU

$$\begin{cases}
a_k = 1 \text{ AU} \\
e_k = \left(1 + \frac{2}{\sqrt{3}}\xi + \frac{4}{3}\xi^2 \right)^{1/2} - 1 \\
\tan i_k = \frac{\xi}{1 + \xi/\sqrt{3}} \\
\omega_k = \frac{\pi}{2} \\
\Omega_k = \frac{2}{3}\pi(k-1) - \frac{\pi}{2} \\
M_k(t) = 2\pi t - \frac{2}{3}\pi(k-1) - \pi,
\end{cases} \quad (4)$$

where $\xi = l/(2a_k) \simeq 1.67 \times 10^{-2}$ and $M_k(t)$ is the mean anomaly. Such orbits minimize the variation of the inter-spacecraft distance between the i -th and j -th satellite $\Delta L_{i,j} \equiv |\mathbf{r}_i(t) - \mathbf{r}_j(t)|$ [12], which turns out to be independent of time at the first order in ξ [8]. This requirement must be fulfilled in order to operate LISA successfully. In fact, the measured quantities for the GW searches are the differential relative motion between the couples (i, j) and (j, l) of the three reference masses, $\delta L_{i,j,l} = \Delta L_{i,j} - \Delta L_{j,l}$ (see Fig. (1)). Each couple can be regarded as an unequal arm interferometer and the doppler shift induced by the relative differential motions can be measured by a suitable Time Delay Interferometry (TDI) [1] with a strain sensitivity in Fig. (2) [4].

The keplerian motions of the LISA reference masses are periodic. We can distinguish their harmonics by looking at the modulus of the Fourier transform of $\delta L_{i,j,l}(t)$ ⁴, as in Fig. (3), where we have considered a finite observation time T and, to overcome the spectral leakage, we have applied a Blackman tapering function [15].

It is worth noticing the absence of the harmonics at 3, 6, 9 ... y^{-1} due to the presence of a discrete symmetry in the equations of motion of the constellation. In fact, as a consequence of the initial conditions in Eq. (4), the LISA triangle rotates as a “quasi-rigid body” with period of one year and, after integer multiples of one third of year, the dynamical configuration is identical to the initial one under any

⁴ The Fourier transform of $F(t)$ is as usual $\tilde{F}(\omega) = \int_{-\infty}^{+\infty} F(t) \exp(-i\omega t) dt$.

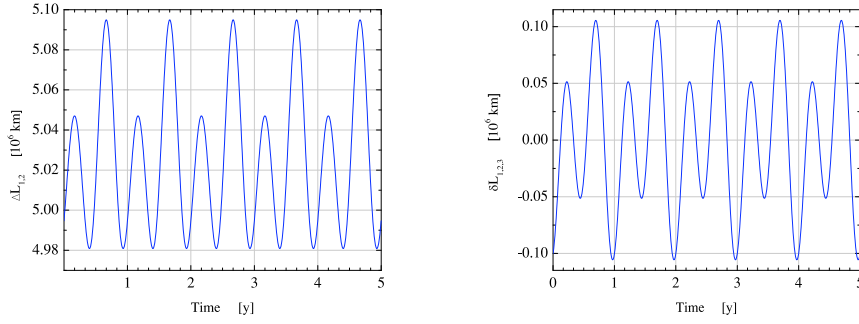


Fig. 1 Left, relative motion of 1 and 2 reference masses $\Delta L_{1,2}$ as a function of time. Right, differential relative motion $\delta L_{1,2,3}$ between couples 1-2 and 2-3 of reference masses as a function of time. For different couples, plots are identical but shifted in time.

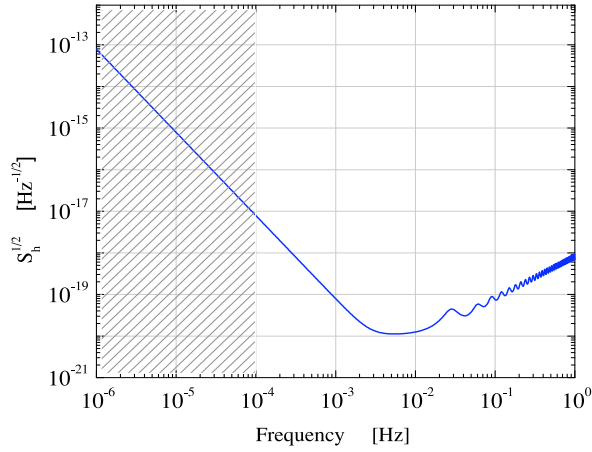


Fig. 2 LISA sensitivity curve as a function of frequency. The curve in the dashed region is calculated from ref. [4], where it is discussed the sensitivity curve up to 10^{-6} Hz.

cyclic permutation of the reference mass indices. However, such a feature is only of theoretical interest, because slightly different initial conditions, due for instance to the unavoidable injection errors of LISA spacecrafts in their orbits (position $\simeq 2$ Km and velocity $\simeq 2$ mm/s, [17]), will produce harmonics of the 3 y^{-1} frequency.

To study the effects of ID on LISA orbits, we apply the perturbation theory in the six-dimensional space of parameters and use the Gauss planetary equations. Such equations provide time evolution of the orbital parameters under a generic perturbing

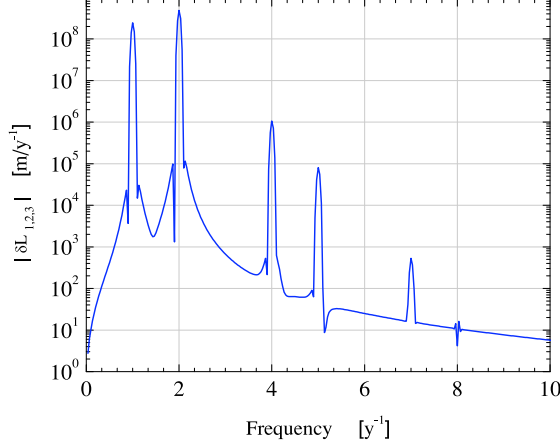


Fig. 3 $|\widetilde{\delta L}_{1,2,3}(\omega)|$ windowed by a Blackman function with $T = 30$ y ($1 \text{ y}^{-1} \approx 3.1709792 \times 10^{-8}$ Hz).

acceleration field $\boldsymbol{\gamma}(\mathbf{r})$ and read

$$\left\{ \begin{array}{l} \frac{da_k}{dt} = \frac{2}{n_k \sqrt{1-e_k^2}} \left[e_k A_r \sin \theta_k + A_t \left(\frac{p_k}{r} \right) \right] \\ \frac{de_k}{dt} = \frac{\sqrt{1-e_k^2}}{n_k a_k} \left\{ A_r \sin \theta_k + A_t \left[\cos \theta_k + \frac{1}{e_k} \left(1 - \frac{r}{a_k} \right) \right] \right\} \\ \frac{di_k}{dt} = \frac{1}{n_k a_k \sqrt{1-e_k^2}} A_n \left(\frac{r}{a_k} \right) \cos(\omega_k + \theta_k) \\ \frac{d\Omega_k}{dt} = \frac{1}{n_k a_k \sin i_k \sqrt{1-e_k^2}} A_n \left(\frac{r}{a_k} \right) \sin(\omega_k + \theta_k) \\ \frac{d\omega_k}{dt} = -\cos i_k \frac{d\Omega_k}{dt} + \frac{\sqrt{1-e_k^2}}{n_k a_k e_k} \left[-A_r \cos \theta_k + A_t \left(1 + \frac{r}{p_k} \right) \sin \theta_k \right] \\ \frac{dM_k}{dt} = n_k - \frac{2}{n_k a_k} A_r \left(\frac{r}{a_k} \right) - \sqrt{1-e_k^2} \frac{d\omega_k}{dt} \end{array} \right. \quad (5)$$

where $p_k = a_k(1-e_k^2)$ is the semi-latus rectum, θ_k is the true anomaly, $n_k = \sqrt{4\pi^2/a_k^3}$ is the keplerian mean motion and A_r, A_t and A_n are the components of $\boldsymbol{\gamma}$ along the versors $\hat{r} = \mathbf{r}/\|\mathbf{r}\|$ in the radial direction, \hat{t} , orthogonal to \hat{r} in the osculating plane and in the direction of $\dot{\mathbf{r}}$, and $\hat{n} = \hat{r} \times \hat{t}$ [6].

For the generic point $\mathbf{r} = (x, y, z)$ close to the ecliptic plane ($i_k \approx 10^{-2}$ rad $\forall k$), the accelerating field $\boldsymbol{\gamma}(\mathbf{r})$ has been calculated from the internal gravitational potential of the distribution in Eq. (2),

$$\Phi(R, z) = \varphi \sum_{n=0}^{\infty} \binom{1 - \frac{\alpha}{2}}{n} \times \\ \times \int_0^{\infty} \left(\frac{R^2}{\tau + a^2} \right)^{1 - \frac{\alpha}{2}} \left[\frac{\tau + a^2}{R^2} \frac{1}{\tau + b^2} \right]^n \frac{z^{2n}}{(\tau + a^2) \sqrt{\tau + b^2}} d\tau, \quad (6)$$

where $R = \sqrt{x^2 + y^2}$, $\varphi = 2\pi\rho_0 Gr_0^\alpha a^{3-\alpha} \sqrt{1 - \gamma_E^2 / (1 + \gamma_E^2)} / (2 - \alpha)$ and G is the Newton gravitational constant. The gravitational potentials of the considered distributions can be easily obtained for the appropriate values of α and γ_E .

We then numerically integrated the Gauss equations for the three LISA satellites adopting different ID distributions⁵. In order to check the effectiveness of the linear perturbation theory of the studied perturbations, we have compared our results with the numerical solutions obtained by keeping the orbital elements on the RHS unperturbed, and they matched exactly within the integration time (30 years). In addition, the accuracy of the numerical integrations ($\approx 10^{-30}$) have been verified by comparison with analytical solutions of Gauss equations (approximated to the fourth order in e and with unperturbed orbital parameters on the RHS) for a spherical homogeneous distribution of matter [7] and the agreement has been satisfactory. To get the perturbed orbits, and, therefore, the perturbative effects of ID on LISA constellation, we substituted the unperturbed orbital parameters appearing in Eq. (3) with the solutions of Eq. (5).

4 Results

In Fig. (4), we report the plot representing

$$\delta l_{1,2,3} = \delta L_{1,2,3}^{pert} - \delta L_{1,2,3}^{unpert}, \quad (7)$$

i.e., the difference between perturbed and unperturbed differential motions of the constellation for the four considered distributions.

We note that the perturbative effects of ID are very small, in fact the LISA constellation opens with an amplitude of the order of $10^2 \mu\text{m}$ after 5 complete orbits. Fig. (5) shows the modulus of the Fourier transform of the difference between perturbed and unperturbed differential motions $\delta l_{1,2,3}$, for the ellipsoidal ID distribution with radial profile, and we see that ID enhances resonance peaks, in particular the 2 y^{-1} harmonic. In addition, new harmonics corresponding to integer multiples of 3 y^{-1} appear, as a consequence the ID gravitational field that breaks the permutation symmetry of the equations of motion.

Therefore, our analysis for the different ID distributions listed at the end of Sec. (2) shows that curves in Fig. (4) and Fig. (5) change their amplitudes of a factor ≈ 2.5 by varying γ_E from $\sqrt{3}$ to 0, while they do not depend significantly on α . Additionally, it is easy to show that LISA sensitivity curve is not significantly affected by the ID perturbing effects in the $10^{-4} - 10^{-1}$ Hz frequency band.

⁵ We made use of the *Mathematica 7* numerical integrator *NDSolve*; see the documentation webpage <http://reference.wolfram.com/mathematica/ref/NDSolve.html>

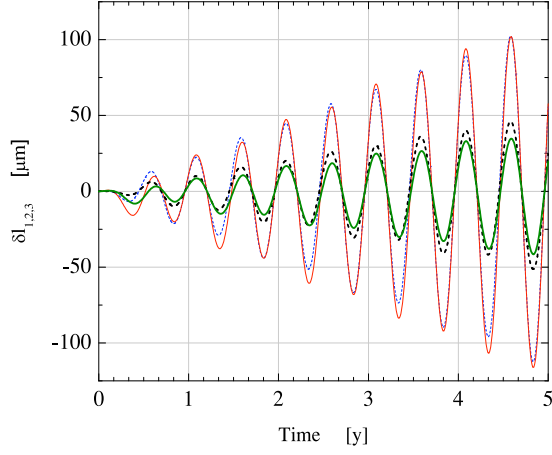


Fig. 4 (color on line) Time evolution of $\delta l_{1,2,3}$, for the spherical ($\gamma_E = 0$) distribution (thin dashed line, $\alpha = 0$, thin solid line, $\alpha = 1.3$) and ellipsoidal ($\gamma_E = \sqrt{3}$) (thick dashed line, $\alpha = 0$, thin solid line, $\alpha = 1.3$) distribution. It is worth noticing that ID induces effects of the order of $10^2 \mu\text{m}$, 10^{12} times smaller than those due to the keplerian differential motions.

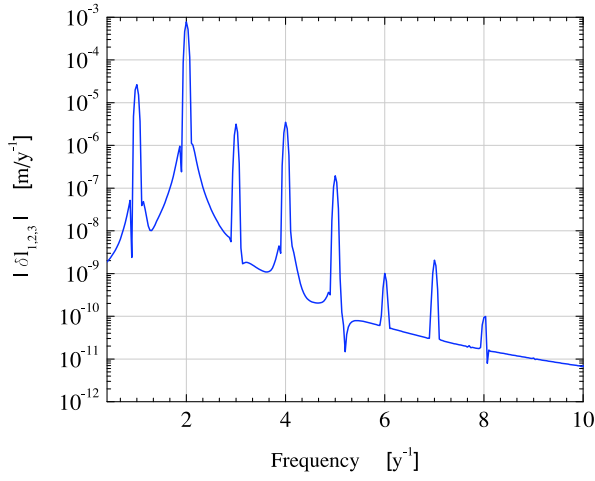


Fig. 5 Difference between $\delta L_{1,2,3}^{pert}$ and $\delta L_{1,2,3}^{unpert}$ spectra of frequencies after 30 orbits, windowed with Blackman function, obtained with $\alpha = 1.3$ and $\gamma_E = \sqrt{3}$; we note the presence of the harmonics corresponding to the integer multiples of 3 y^{-1} , contrary to Fig (3).

4.1 Optimal ID signal resolution

It is of some interest to investigate the problem of resolving the contributions to the differential relative motions due to Sun and ID by means of optimal filtering. From the theory of signals resolution we know that if a noisy signal $v(t)$ can be a linear combination of two given signals $f(t)$ and $g(t)$ of unknown amplitudes A and B

$$v(t) = Af(t) + Bg(t) + n(t), \quad (8)$$

where $n(t)$ is a zero mean gaussian stochastic process with correlation $\langle n(t)n(t') \rangle = S_0\delta(t-t')$, the four following hypothesis are possible:

1. H_0 : neither signal A nor signal B is present;
2. H_1 : signal A alone is present;
3. H_2 : signal B alone is present;
4. H_3 : both signal A and B are present,

which are to be verified by comparing the expectation values of A and B , with zero (test of hypothesis). The best estimate of A and B turns out to be [11]

$$\begin{aligned} \hat{A} &= \frac{1}{1-\lambda^2} \int_0^T [f(t) - \lambda g(t)] v(t) dt \\ \hat{B} &= \frac{1}{1-\lambda^2} \int_0^T [g(t) - \lambda f(t)] v(t) dt, \end{aligned} \quad (9)$$

with standard deviations

$$\sigma_{\hat{A}} = \sigma_{\hat{B}} = \frac{S_0^{1/2}}{\sqrt{2(1-\lambda^2)}}, \quad (10)$$

where $\lambda = \int_0^T f(t)g(t)dt$, S_0 is the noise power density and $f(t)$ and $g(t)$ are normalized to unit energy, $\int_0^T f^2(t)dt = \int_0^T g^2(t)dt = 1$.

In our case, $v(t)$ represents the perturbed differential motions, $Af(t)$ and $Bg(t)$ are the contributes due to Sun and ID respectively. We stress that $f(t)$, $g(t)$, \hat{A} and \hat{B} are almost independent of the initial conditions of LISA reference masses. It is worth noticing that the two contributions to the perturbed motion are almost orthogonal, ($\lambda \simeq 10^{-2}$) as can be seen in Fig. (6), where the normalized functions $f(t)$ and $g(t)$ are plotted.

As a crude estimation, a strain sensitivity $S_h \approx 10^{-11} 1/\sqrt{\text{Hz}}$ at the 2 y^{-1} ($\approx 6.4 \cdot 10^{-8} \text{ Hz}$) frequency (the most powerful ID harmonic), is required to achieve a unitary signal-to-noise ratio ($\text{SNR} = \hat{A}/\sigma_{\hat{A}} = \hat{B}/\sigma_{\hat{B}}$.) in a 5 years observation time. However, in the literature there exist extrapolations of the strain sensitivity S_h only up to 10^{-6} Hz [4] and the measure of such a small signal amplitude depends on the noise level of LISA at very low frequencies (10^{-7} Hz), which is still largely unknown.

5 Discussion

We have calculated the ID perturbing effects on the LISA differential motions. Using the estimated ID density, we found a continuous opening of the LISA orbits of the

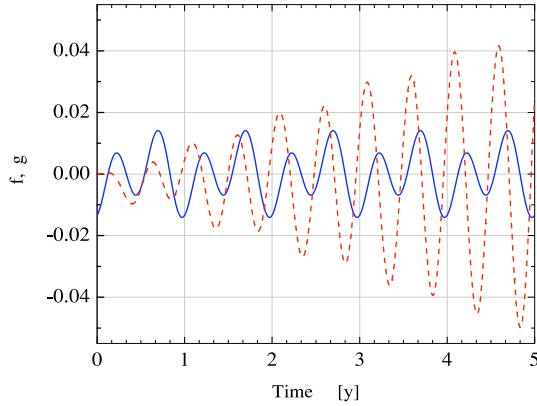


Fig. 6 (color on line) Time evolution of the two normalized functions $f(t)$ (blue solid line) and $g(t)$ (red dashed line) for the case of an ellipsoidal distribution with radial profile.

order of $10^2 \mu\text{m}$ after 5 years at 2 y^{-1} frequency. Moreover, due to the particular LISA orbits, which are nearly circular and very close to the ecliptic plane, we found similar effects for the distributions we have taken into account. In fact, the ID tidal forces vary significantly over a scale much larger than the LISA triangle sides.

All the results we presented for ID also hold in the presence of LDM. In fact, we have shown that the numerical solutions of Eq. (5), for the LISA orbits, are almost independent on α and γ_E parameters within the investigated range and of the injection errors. In addition, the perturbations on LISA relative differential motions $\delta L_{i,j,k}$ scale linearly with ρ_0 . Thus we can account for LDM just by a rescale of ρ_0 : for instance, if we assume that the LDM density value is close to the average galactic dark matter (GDM) density value, $\rho_{0,GDM} = 5 \cdot 10^{-22} \text{ kg/m}^3$ as obtained from the galaxy rotation curve, the effect of DM is expected to be 0.5% that of ID.

As a consequence, LISA could provide interesting upper limits on both $\rho_{0,ID}$ and $\rho_{0,LDM}$, depending on low frequencies noise and ρ_0 value, by means of direct gravitational field measurements instead of observations of zodiacal light in the case of ID. At present time, the best upper limits $\rho_{0,LDM} < 3 \cdot 10^{-16} \text{ kg/m}^3$ are based on the study of the precession of the perihelions of Mercury, Earth and Mars [13].

However, we stress that a thorough study of LISA displacement noise below $1 \mu\text{Hz}$, including local gravitational field fluctuations, thruster noise, orbit determination and injection errors [5] etc., is required to establish the relevance of the ID effects in LISA physics.

6 Conclusions

The study of the Solar System gravitational field acting on LISA reference masses is of some relevance also for the detection of GWs. In fact, the non-radiative gravitational perturbations on LISA keplerian motions must be subtracted at the highest accuracy

from the relative differential motion in order to measure the GW contributions. In this paper we have calculated the time evolutions of the orbital parameters due to some ID distributions and estimated the opening induced on the LISA constellation, $\approx 10^2 \mu\text{m}$ after 5 years. The Fourier transform of the perturbation of the differential relative motion has shown an enhancement of the resonances characterizing the unperturbed spectra, in particular the peak at 2 y^{-1} frequency. As a consequence of the LISA orbits, such effects are similar for the studied distributions of ID and do not affect the LISA sensitivity band for GW detection.

On the other hand, the discrimination of very small perturbations from the keplerian differential relative motion depends crucially on the low frequency displacement noise, that in the ideal case should be $\simeq 10^{-11} 1/\sqrt{\text{Hz}}$ at 2 y^{-1} frequency to detect ID at the density $\sim 10^{-20} \text{ kg/m}^3$ measured by the zodiacal light. Unfortunately, a reliable estimate of this noise level at very low frequency is still lacking and requires further investigations.

Finally, we investigate the possibility of constraining the LDM density with LISA. Even though gravitational perturbations due to ID and LDM are undistinguishable, the study of the deviations from the keplerian orbits of LISA reference masses could provide interesting upper limits on LDM density.

7 Acknowledgments

MS was supported by the Swiss National Science Foundation and the Dr. Tomalla Foundation. GM was supported by the Italian INFN (Istituto Nazionale di Fisica Nucleare). MC and GM are grateful to Professor G. Benettin for useful discussions.

References

1. Armstrong, J.W. *et al.*: 2003, ‘Time delay interferometry’ *Class. Quantum Grav.* 20, 283-289.
2. Bender, P. *et al.*: 1998, ‘Pre-Phase A Report’, second edition.
3. Bender, P. *et al.*: 2000, ‘LISA: a cornerstone mission for the observation of gravitational waves System and Technology Study’, Report ESA-SCI 11.
4. Bender, P.: 2003, ‘LISA sensitivity below 0.1 mHz’, *Class. Quantum Grav.* 20, 301-310.
5. Bik J.J.C.M. *et al.*: 2007, ‘LISA satellite formation control’, *Advances in Space Research* 40, 25-34.
6. Boccialetti, D. and Pucacco, G.: 2001, *Theory of orbits* Springer, Berlin.
7. Cerdonio, M. *et al.*: 2009, ‘Local Dark Matter searches with LISA’, *Class. Quantum Grav.* 26, 094022.
8. Dhurandhar, S.V. *et al.*: 2005, ‘Fundamentals of the LISA stable flight formation’, *Class. Quantum Grav.* 22, 481-487.
9. R.H. Giese *et al.*: 1986, ‘Three-dimensional models of the zodiacal dust cloud: a comparative study’, *Icarus* 68, 395-411.
10. E. Grün *et al.*: 1985, ‘Collisional balance of the meteoritic complex’, *Icarus* 62, 244-272.
11. Helstrom, C.W.: 1960, *Statistical theory of signal detection*, Pergamon Press, New York.
12. Jiang, F. *et al.*: 2007, ‘Approximate analysis for relative motion of satellite formation flying in elliptical orbits’, *Celestial Mech Dyn Astr* 98, 31-66.
13. Khirplovic, I.B. and Pitjeva, E.V.: 2006, ‘Upper limits on density of dark matter in Solar System’, *Int. J. Mod. Phys.* 15, 616-618.
14. Levasseur-Regourd, A.C., 1996, ‘Optical and Thermal Properties of Zodiacal Dust”, *Physics, Chemistry and Dynamics of Interplanetary Dust*, ASP Conference series 104, 301-308.
15. Proakis, J.G. and Manolakis, D.G.: 1992 *Digital signal processing* Macmillan Publishing Company, second edition, New York.

16. Sereno, M. and Jetzer, Ph.: 2006, 'Dark matter versus modifications of the gravitational inverse-square law: results from planetary motion in the Solar system' *Mont. Not. R. Astron. Soc.* 371, 626-632.
17. Sweetser, T.H.: 2005, 'An end-to-end description of the LISA mission', *Class. Quantum Grav.* 22, 429-435.